Measurement of Residence Time Distribution in a Rotary Calciner

Yijie Gao, Benjamin J. Glasser, Marianthi G. Ierapetritou, Alberto Cuitino, and Fernando J. Muzzio
Dept. of Chemical and Biochemical Engineering, Rutgers University, Piscataway, NJ 08854

Jean W. Beeckman, Natalie A. Fassbender, and William G. Borghard
Process Research Laboratories, ExxonMobil Research & Engineering, Annandale, NJ 08801

DOI 10.1002/aic.14175
Published online July 9, 2013 in Wiley Online Library (wileyonlinelibrary.com)

Rotary calcination is widely used in catalyst manufacturing and many other industrial processes. In this article, the influence of operational variables and material properties on the mean residence time (MRT), hold up, and axial dispersion was investigated in a pilot plant rotary calciner. Residence time distributions (RTD) of spherical, cylindrical, and quadrilobe catalyst particles were measured and contrasted. The Saeman's model was successfully applied to predict the experimental bed depth and the MRT as particles flowed through the calciner. It was observed that increasing the feed rate did not significantly affect the MRT. Results for the different particles indicated that cylinders and quadrulobes exhibited less axial dispersion than spheres due to the decreased flowability. A reliable method was developed to provide a reasonable RTD prediction in rotary calcination systems. © 2013 American Institute of Chemical Engineers *AIChE J*, 59: 4068–4076, 2013

Keywords: rotary calciner, alumina, residence time distribution, particulate flow, dispersion

Introduction

Rotary drums are one of the most commonly used continuous solid handling devices in chemical and metallurgical manufacturing. They can be used to perform versatile operations such as blending, heating, drying, sintering, calcination, and gas-solid reactions of a variety of feed stocks.[1] The material to be treated is fed into an inclined cylindrical drum and transported forward due to slow rotation of the drum. During this mass transport process, the material exchanges heat with the wall and the freeboard gas. If the material to be treated does not come predried, the calciner has a short drying zone.[2] This is followed by a heating zone to bring the material up to the reaction temperature, which may occupy a significant portion of the drum length, and a short reaction zone at the end.[1] Most recent studies have generally focused on the bed heat transfer, although reaction kinetics have also been included into the models for specific reaction cases.[3–7]

Although the focus of this work is the axial mass transfer in rotary drum, previous literature about heat transfer in this process is also summarized as follows. Heat-transfer models have been developed for the bed material, freeboard gas, and refractory wall in the cross-sectional plane and along the axial direction.[8] In high-temperature cases, radiation from the freeboard gas and walls is the most important heat-transfer mechanism. Boateng and Barr[9] incorporated a two-dimensional representation of the bed's transverse plane into a conventional one-dimensional plug flow model, which was able to predict the heat transfer from the freeboard gas to the material bed. In another paper by Boateng and Barr,[10] segregation was investigated for particles with different sizes, and the resulting segregated state was used to estimate the effective thermal conductivity of the bed. Studies by Dhanjal et al. [11] suggested that segregation has little influence on heat transfer within the bed and the radial thermal gradients are primarily the result of improper particle blending. For low to medium temperatures, heat transfer from the covered wall to the material bed is the dominant mechanism, while transfer from the exposed wall and freeboard gas to the active layer accounts for only a small fraction of heat transfer.[12] Li et al. [13] extended a penetration theory by considering the effect of rotation to describe the heat-transfer coefficient of the covered wall to the bulk solid.

Particle dynamic simulations have been productively used to investigate granular flows in a variety of situations.[14,15] The simplicity of the calcination operation—a rotating cylinder with particles—lends itself particularly well to particle dynamics simulations.[16,17] Particle dynamic simulations were applied to investigate the flow and heat transfer between the wall and the bulk particles for a rotary calciner. Simulations and experimental validation showed that rotary speed has little impact on the wall-particle heat transfer. Similar experimental results were observed in the study of a novel experimental apparatus for temperature measurements.[18] It was found that the solid-to wall heat-transfer coefficient increases linearly with the solid flow rate but shows negligible variation with the rotary speed. A new 3-D temperature measurement system consisting of thermocouple arrays was

Correspondence concerning this article should be addressed to F. J. Muzzio at fjmuzzio@yahoo.com.

developed,[19] which can be used to obtain data over a wide range of operating conditions.

Besides the heat-transfer process, the axial residence time of bulk material has been long known to be the other primary factor affecting the performance of a rotary drum[20] and thus is reviewer below. A predictive model has been developed based on the assumption that particles in a rolling bed move in a circular motion with the rotation of the kiln in a passive layer, and then fall down the surface of the bed in a thin active layer.[21] While the time for particles to fall down in the active layer is small compared to the time in the passive layer, the bed depth and axial residence time can be predicted using the geometry of the drum and the angle of repose of the bulk material.[22] Sai et al.[23] determined an empirical correlation between operating conditions and mean residence time (MRT) of the material, and established the dam height that leads to a flat bed depth profile. The effect of dam height was further investigated by Scott et al.[24] who considered industrial kilns designed with cylindrical or conical dams at the end or part way along the kiln. An analytical solution to the model equations for the axial mass transport was developed[25,26] which agrees well with the numerical solution of Saeman.[21] The influence of operation parameters and drum geometry on the residence time distribution was investigated.[27,28] Mass hold up was observed to be directly related to feed rate, inversely related to rotary speed, and slightly inversely proportional to angle of inclination.

A number of studies also addressed the particle flow in the transverse plane. Six modes have been identified in a rotating drum: slipping, slumping, rolling, cascading, cataracting, and centrifuging.[29,30] The noninvasive positron emission particle tracking technique was applied to study the transverse velocity field in drums operated at low to medium rotary speed.[31] A novel parameter termed the "solids exchange coefficient" was proposed to model the flux between the passive and active regions. Based on modeling that predicted the transverse bed motion,[29] Liu et al. [32] estimated the critical Froude number for the slumping-rolling transition in a rotary drum. The critical Froude number was found to be proportional to the particle to cylinder diameter size ratio. Heydenrych et al. [33] considered the movement of gas in the interparticle voids in the transverse mass transfer in the rolling mode.

Based on the above review on the previous heat- and mass-transfer studies on rotary drum, the two important time scales for rotary calciner performance are: (1) the characteristic time for heat transfer and calcination in the transverse plane, and (2) the residence time that particles stay inside the system. Desired performance can only be observed when the residence time of the particles inside the calciner is longer than the time necessary for heat transfer and calcination. Therefore, better understanding of the effects of operating conditions, calciner geometry, and material properties on both time scales is critical in providing reliable quality control and process design methods.

Two important aspects of the axial mass transport process were seldom referred in previous literature. First, few studies investigated axial dispersion of particles as plug flow modeling is commonly used to describe axial particle motion. Second, the effect of particle shape on the RTD has not been well studied. To address these issues, in this article, the residence time distribution and bed depth distribution of different types of particles was measured in a pilot scale calciner for various operating conditions. In particular, we focus on the effect of material properties, and operating conditions on the axial dispersion. In general, small value of the axial dispersion coefficient are preferred in catalyst manufacturing, which leads to narrow residence time distribution curves and uniform thermal treatment.

The rest of this article is organized as follows. The "Model" section describes Saeman's model for the prediction of the MRT, and the Taylor's dispersion model for the estimation of the MRT and the axial dispersion coefficient through a RTD fitting process. The "Experimental setting" section introduces the experimental setup of the rotary calciner, as well as RTD and bed depth measurement methods. Then the "Results" section presents the experimental results of the RTD and the bed depth at different conditions, followed by the "Summary" section.

Model

Bed depth distribution and *MRT*

Previous studies indicated the possibility of predicting the bed depth distribution in a continuous rotary drum based on the model proposed by Saeman[21]

$$\frac{dh}{dx}=\frac{3\tan\Theta}{2\omega}\dot{V}\left[R^2-(h-R)^2\right]^{-3/2}-\frac{\tan\beta}{\cos\Theta} \tag{1}$$

where h is the depth of the solid bed, x the axial distance from discharge, and R the radius of the calciner. The model predicts the influence of the dynamic angle of repose Θ of bulk materials, the inclination angle of the calciner β, the volumetric feed rate $\dot{V}$, and the rotary speed ω on the fill level profile in the calciner. The boundary condition of Eq. 1 is the bed depth at the discharge ($x = 0$). For a system with a dam, the bed depth at the discharge is approximately equal to the dam height

$$h(x=0)=h_{\text{dam}} \tag{2}$$

For calciners without a dam, the boundary bed depth equals the average diameter of particles

$$h(x=0)=d \tag{3}$$

While numerical methods can provide very good predictions, current analytical solution approaches derive complicated formulas and have limitations under certain conditions. As a result, a numerical method is applied. The predictive model for the fill level distribution benefits our study as follows:

i. It provides an estimate of the MRT τ. When the bed depth $h(x)$ is predicted, the overall mass hold-up, M, in the calciner and the MRT, τ, can be calculated as

$$M=\rho_s R^2\int_0^L(\varepsilon_x-\sin\varepsilon_x\cos\varepsilon_x)dx \tag{4}$$

$$\tau=\frac{M}{\dot{m}} \tag{5}$$

where ρ_s is the dilated density of particles, ε_x the local fill angle of solids, and $\dot{m}$ the mass feed rate.

ii. It provides an estimate of the time to reach steady state in the RTD measurement. Generally, it takes 1.5–2 times of the MRT to reach steady state.

It should be noticed that the Saeman model is simple but very efficient in capturing axial mass-transfer process in

rotary drum, and thus, is still widely used and discussed in recent literatures.[25,26] Advanced model has been developed after the Saeman's model, most of which were proposed to describe the complicated process of cross-sectional mass transfer. As the purpose of this work is to capture the axial mass transfer (RTD) of rotary drum, the use of more advanced models is not required.

Residence time distribution

The pulse test method developed by Danckwerts[34] is used for the RTD measurement. The implementation we adopted for solids is similar to the previous study by Sudah et al.[28] Bulk material of white alumina is fed into the calciner under constant feed rate. A tracer is made by dyeing some of the alumina with green cobalt oxide. Further details of our particular alumina system is given in the next section. When steady state is reached, the tracer is injected into the stream. Instead of collecting samples at the immediate point of discharge, images are recorded on the outflow stream. Since the tracer can be distinguished from the bulk material by the dye color, the concentration $C(t)$ can be determined as a function of time based on the number of tracer particles in the images. The residence time distribution $E(t)$ is then calculated based on concentration measurements using the following equation

$$E(t)=\frac{C(t)}{\int_{t=0}^{\infty} C(t)dt} \tag{6}$$

To eliminate noise from the RTD measurements and to understand its physical meaning, the RTD measurement is fitted to the Taylor dispersion model[35–37]

$$E(\xi,\theta)=\frac{Pe^{1/2}}{(4\pi\theta)^{1/2}}e^{\frac{-Pe(\xi-\theta)^2}{4\theta}} \tag{7}$$

where $\theta=t/\tau$ and $\xi=x/l$ represent the dimensionless time and location in the rotary calciner, respectively; τ is the MRT, and l is the length from the discharge to the location of tracer injection; $Pe=v_x l/E_x$ is the Peclet number; v_x and E_x are the axial velocity and axial dispersion coefficient, which are estimated from the curve fitting and are used further to understand the effects of operations and material properties on the RTD profiles.

Experimental Setting

Geometry and operations

Experiments were conducted in the 6" rotary calciner covering a wide range of variables at room temperature, as detailed in Table 1. Figure 1 shows the schematic diagram of the experimental pulse test setup. The calciner has an internal diameter of 15 cm (6") and a length of 3.3 m (130"), giving an L/D ratio of 21.7. A screw feeder was used to feed materials to the calciner at a constant rate. The feeder was operated to achieve volumetric feed rates of 75 and 242 cm^3/min. The calciner was operated at rotary speeds of 2, 3.5, and 5 RPM.

Table 1. Range of Operation Variables.

Operation Variables	Conditions
Incline angle (°)	1.8
	2.5
Rotary speed (RPM)	2
	3.5
	5
Volumetric feed rate (cm^3/min)	75
	242

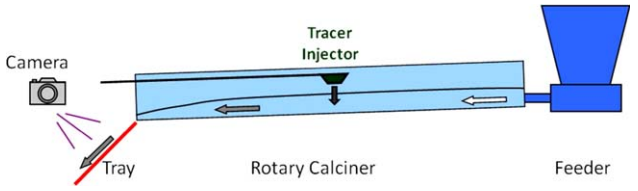

Figure 1. Schematic of the experimental pulse test setup.

[Color figure can be viewed in the online issue, which is available at wileyonlinelibrary.com].

A jack mechanism was provided at the feeder side of the calciner to adjust the incline angle between 1.8° and 2.5°. No dam or lifter was used at the discharge of or inside the calciner, while a fixed circular dam of around 40 mm height was set at the feeder side to avoid backward leakage of materials. The maximum operational fill level without backward leakage is around 20%.

Material

To understand the influence of material properties on the RTD profile, alumina particles with different shape, density, and L/D ratio were used as bulk materials. The spherical particles were supplied by BASF (Iselin, NJ) and are F200 7×14 alumina spheres, with batch number 0200273560 (Spheres). The quadrulobe and cylindrical alumina particles are typically applied in homogeneous deposition precipitation catalyst, denoted as 1/20 Quadrulobe and 1/16 Cylinder, respectively. All of the particles are γ-alumina (Figure 2). Table 2 shows detailed material properties of the three kinds of particles. As listed in the table, angle of repose of the spheres is smaller than the other materials, indicating better flowability, thus lower residence time is expected inside the calciner. For the RTD experiments of each material, the corresponding tracer was prepared by dyeing the same bulk material with cobalt oxide. Material properties such as dilated density and angle of repose were also measured for the tracer and they were found to be unchanged from the original bulk material.

Pulse test

Under steady-state conditions, a spoon-like tool with a long handle was used, inserted into the calciner, and the tracer was injected into the bulk material at a location 1.5 m (60") from the discharge (Figure 1). Images of particle flow were recorded on the tray by a Canon A520® camera. The total number of tracer particles in every five or ten images, taken with a time interval of 2 s, was counted manually. Experiments were carried out using different amounts of tracer in order to determine the reproducibility of the RTD (see Figure 3). The quantity of tracer used for each pulse test was chosen to be 50 cm^3, due to a good RTD reproducibility under that condition (see Figure 3b).

Bed depth distribution

The bed depth at different axial positions along the calciner was measured using a ruler attached to the end of a

Figure 2. Bulk materials of alumina.

(a) Sphere. (b) Cylinder. (c) Quadrilobe.

6-foot rod. Under steady-state conditions, the calciner and feeder were stopped, and the rod was inserted into the calciner. The ruler was then made to touch the bottom of the calciner through the bed, and the value on the ruler was recorded. This procedure was repeated for different axial distances of 2", 4", 6", 12", 24", and 36" from the discharge.

Results

Prediction of bed depth distribution and MRT

To verify Saeman's model described in the "model" section, bed depth distribution and MRT were predicted by applying Eqs. 1–5 with the operation and material properties in Tables 1 and 2.

Figure 4 shows the comparison between the predicted and experimental data of bed depth distribution for all three alumina materials at room temperature. The measurements were performed at rotary speed of 5 RPM and incline angle of 2.5° for both feed rates. The solid lines in the plots denote the model predictions; the circle and cross points indicate experimental measurements. As can be seen from Figure 4, an increase of feed rate leads to a higher hold-up at constant rotary speed and incline angle. Higher hold-up is also observed as angle of repose increases from sphere to cylinder and quadrilobes. Figure 5 plots the comparison of predicted and experimental MRT. It is apparent that MRTs in the cases of sphere and cylinder are somewhat overestimated. This may result from attrition inside the feeder, which introduces alumina fines due to the small distance (around 1 mm) between the screw and the sidewall. While the overall hold-up of the calciner may not be significantly influenced by the fines, the effective hold-up occupied by particles is smaller. This may lead to a smaller experimental MRT. Despite attrition, the results in both Figures 4 and 5 show fairly good predictions, indicating the applicability of Saeman's model for design and quality control of continuous calcination processes.

Effect of material properties and process variables

Figure 6 shows the effect of process variables (volumetric feed rate, rotary speed, and incline angle) on the residence time distributions of spheres (SPH-RT), cylinders (CYL-RT), and quadrilobes (QUAD-RT) at room temperature. Observations from Figure 6 include: (1) MRT increases from spheres to cylinders and quadrilobes, due to an increasing angle of repose; (2) particles stay longer in the calciner when the drum rotation is slower or incline angle is smaller; (3) influence of feed rate on the MRT is not as significant as the other operations; (4) axial dispersion is lower at the higher feed rate in the sphere cases; while for the other two materials, feed rate hardly influences axial dispersion.

To better clarify the effect of operations and material difference, Figure 7 summarizes the fitted values of axial dispersion coefficient E_x (subplots 7a–7c) and MRT τ (subplots 7d–7f). These values are obtained from the fitting the Taylor dispersion model. The corresponding average fill levels predicted from Saeman's model are also plotted (subplots 7g–7i).

As subplots 7a–7c show, axial dispersion coefficients of particles are limited to the range 0–5 cm^2/min for most conditions, except for the sphere cases at the lower feed rate. For spheres one can also see that dispersion is larger at larger incline angle. This results from the lower fill level due to the lower angle of repose of the spheres (improved flowability). At the higher feed rate, we hypothesize that the increased fill level limits the position exchange of neighboring spheres and leads to a lower dispersion coefficient. For the other two materials, the larger L/D ratio (4.3 for cylinders and 5.3 for quadrilobes) results in interlocking between neighboring particles, which makes particles difficult to disperse even when the fill level is low. Dispersion was further limited in the quadrilobe cases (subplot 7c), and we hypothesize that the approximate square cross section of the quadrilobe leads to more stable interlocking than the circle cross section of cylinder particles. As with observations from Figure 6, subplots 7d–7f depict an increasing MRT from spheres to cylinders and quadrilobes, following the increase of predicted fill level in subplots 7g–7i.

A uniform treatment of particles in the calciner corresponds to a narrow RTD. This in turn corresponds to a large Peclet number: $Pe=v_x l/E_x$ where v_x and E_x are the axial velocity and axial dispersion coefficient respectively. Our results suggest that in order to achieve a narrow RTD profile, an effective adjustment is to increase the feed rate, which leads to a decrease in the axial dispersion coefficient while

Table 2. Physical Properties of Tracer and Bulk Materials

Material	Dilated Density (g/cm3)	Length (mm)	Diameter (mm)	Angle of Repose (°)
Sphere (SPH)	0.8	-	1.62 ± 0.33	21.1
Cylinder (CYL)	0.6	6.76 ± 3.12	1.62 ± 0.37	34.3
Quadrilobe (QUAD)	0.47	5.04 ± 2.39	1.26 ± 0.12	31.4

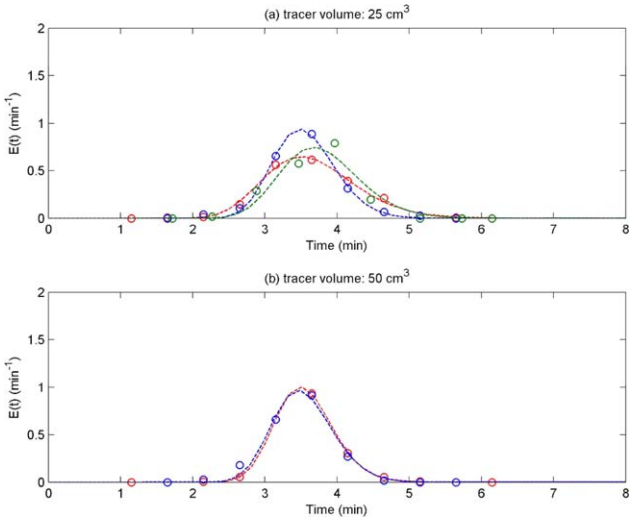

Figure 3. RTD reproducibility of spheres with different tracer quantities.

(a) 25 cm^3. (b) 50 cm^3. Operating conditions: feed rate 75 cm^3/min, rotary speed 5 RPM, incline angle 2.5°. [Color figure can be viewed in the online issue, which is available at wileyonlinelibrary.com].

keeping a constant MRT (leading to a larger Peclet number). Notice that the influence of increasing the feed rate on transverse heat transfer should also be considered since the fill level increase with an increase of feed rate. Meanwhile, adjusting rotary speed or incline angle does not work very well, in terms of a narrow RTD since our results show that adjusting the rotary speed or incline angle to decrease axial

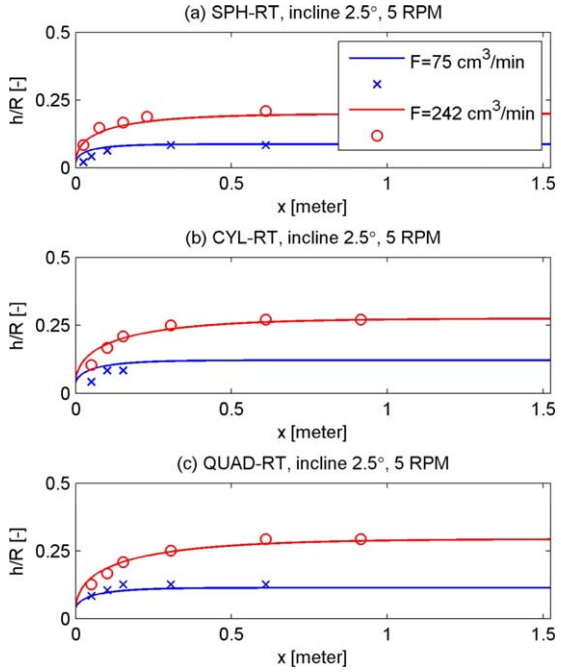

Figure 4. Comparison of predicted and experimental bed depth distribution at RT.

(a) spheres, (b) cylinders, (c) quadrilobes. h/R: bed depth normalized by the inner radius of calciner; x: axial distance from the discharge. [Color figure can be viewed in the online issue, which is available at wileyonlinelibrary.com].

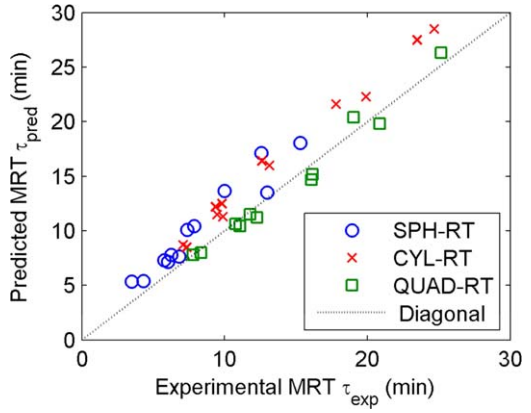

Figure 5. Comparison of predicted and experimental MRT distribution.

[Color figure can be viewed in the online issue, which is available at wileyonlinelibrary.com].

dispersion can result in larger MRT, which counterbalances the effect of limiting axial dispersion.

In summary, larger MRT and smaller axial dispersion coefficient are observed in the cases of cylinders and quadrulobes, especially for the conditions of low rotary speed and small incline angle. The results summarized above can serve as guide in design and quality control of the continuous calcination process.

Effect of Particle size and L/D ratio

A distribution of particle sizes or L/D ratios is a common situation in industrial processes and solids handling.[38] To understand the influence of particle size and shape on RTD profiles, two additional tests were performed. In the first test, one RTD pulse test for the spheres was analyzed for particle size differences between the beginning, middle and end of the RTD. Images were separated into three partitions for different residence times of the tracer particles: partition I represents residence times smaller than 15 min; partition II represents residence times between 15 and 15.6 min; partition III represents residence times larger than 15.6 min. The range of residence times was set so that around 100 tracer particles were observed for images within each partition. Particle-size distributions of these partitions were determined and plotted in Figure 8, in which the average sphere diameter is around 2 mm in partition I, 1.2 mm in partition II, and 0.8 mm in partition III. Results show that smaller particles have a longer residence time inside the calciner. One possible reason for this phenomenon is segregation of particles due to different particle size. Previous work has shown that large particles tend to ride onto the bed surface in the calciner, while small particles together with fines due to attrition in the feeder are more likely to stay in the kidney core region in the elliptic section of the bed.[10] We hypothesize that when larger particles are more likely to be on the active layer and fall faster on the surface in the transverse plane, they also move faster along the calciner in the axial direction, which leads to shorter residence time.

The effect of the L/D ratio can be illustrated in the second test, in which both bulk material and tracer of the original cylinders (average L/D ratio 4.1) were screened to a top cut (average L/D 5.0) and bottom cut (average L/D 4.0). Additional pulse tests were performed for both for an incline

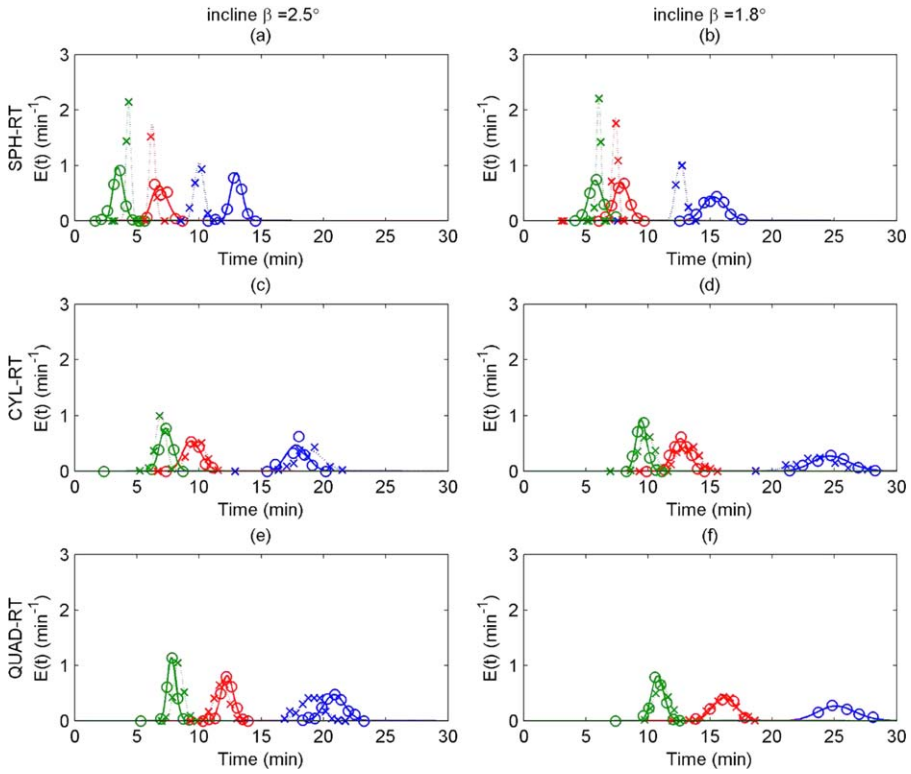

Figure 6. Experimental RTD data and fitted curves.

Open circle: 75 cm^3/min; cross: 242 cm^3/min. Blue: 2 RPM, red: 3.5 RPM; green: 5 RPM. [Color figure can be viewed in the online issue, which is available at wileyonlinelibrary.com].

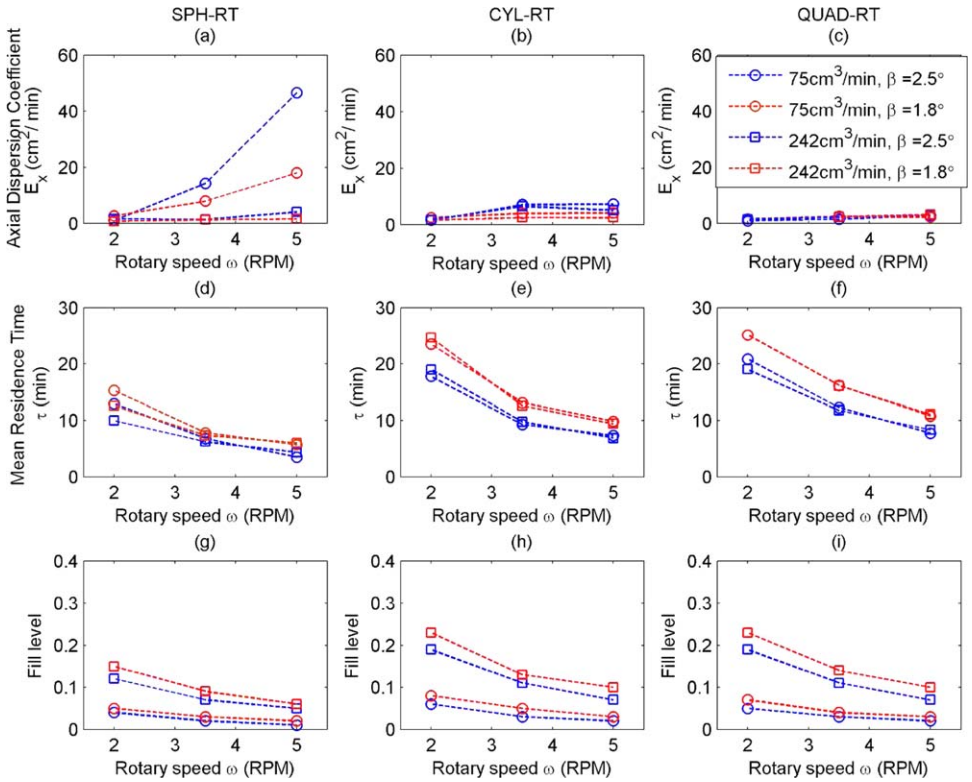

Figure 7. Fitted values of axial dispersion coefficient (a–c), MRT (d–f), and predictions of average fill level (g–i).

[Color figure can be viewed in the online issue, which is available at wileyonlinelibrary.com].

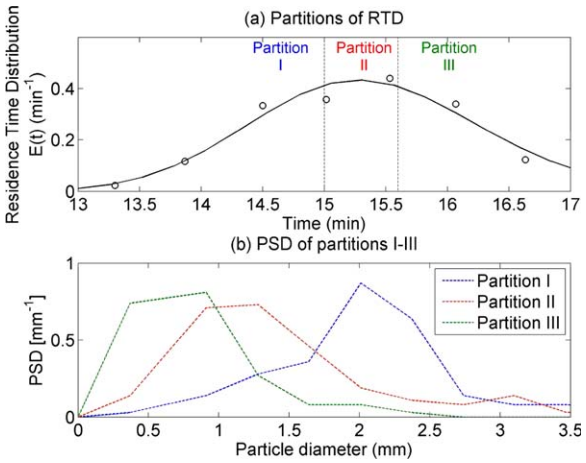

Figure 8. Size distribution of tracer particles with different residence time.

(a) Partitions of RTD. (b) Particle-size distribution of different partitions. Test conditions: sphere alumina; feed rate 75 cm^3/min; incline angle 1.8°; rotary speed 2 RPM. [Color figure can be viewed in the online issue, which is available at wileyonlinelibrary.com].

angle of 2.5° and rotary speed of 5 RPM. Figure 9 shows the results of the RTDs and fitted results of these additional cases, compared to the original one. For a feed rate of 75 cm^3/min, the cases of the original cylinders (unscreened) and the bottom cut (bot-cut) show similar RTD and fitted parameters, while MRT of the top-cut case is slightly larger. Since the bottom cut and unsieved material have a similar L/D ratio it is not surprising that they have similar RTDs. We hypothesize that the larger MRT for the top cut is due to decreased flowability at larger L/D ratio.

RTD prediction

One goal of this work was to develop a reliable method to predict RTD in a calciner. Based on previous work,[25] Saeman's model provides accurate prediction of one of the key parameters of RTD: the MRT. For the other key parameter, the axial dispersion coefficient, previous work did not provide a quantitative predictive method,[28] since the axial dispersion coefficient largely depends on material shape. However, since low axial dispersion is preferred in the calcination process, we

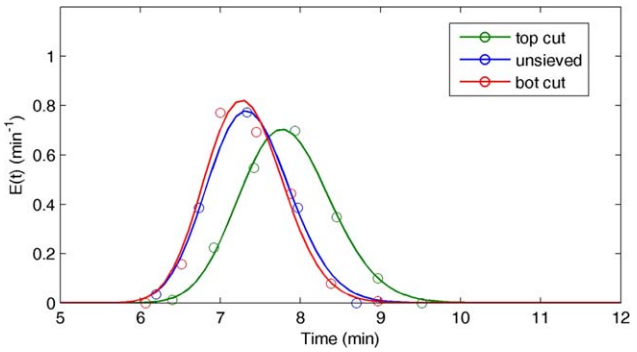

Figure 9. RTD profiles of alumina cylinders with different L/D ratio.

Test conditions: alumina cylinders; feed rate 75 cm^3/min; incline angle 2.5°; rotary speed 5 RPM. [Color figure can be viewed in the online issue, which is available at wileyonlinelibrary.com].

are interested in materials or conditions in which dispersion is limited. This makes it possible to predict RTD profiles.

Figure 10 compares data and predictions of RTDs except the sphere cases with large axial dispersion coefficient (low feed rate). We observed that the axial dispersion coefficients for spheres at the low feed rate are significantly larger than that for the other cases. As limited axial dispersion is preferred, we focused on the RTD of all of the cases (spheres at high feed rate, cylinders, and quadrulobes) except the sphere cases at low feed rate. This was accomplished by estimating the MRT (for the predicted curves) from Saeman's model. The axial dispersion coefficients were estimated based on the following observations from Figures 6 and 7a–c: (1) the axial dispersion coefficient did not vary significantly with feed rate and incline angle; (2) the axial dispersion coefficient varied with rotary speed; (3) the axial dispersion coefficient did not change significantly for different materials (spheres at high feed rates, cylinders, and quadrulobes); (4) limited variation of the small axial dispersion coefficient (between 0–10 cm^3/min) did not influence the RTD profile significantly. Based on these observations, the axial dispersion coefficients were arbitrarily estimated as 2, 3, 4 cm^2/min for rotary speed of 2, 3.5, 5 RPM (Figure 11). Although Figure 10 do not show a perfect fit, they provide reasonable prediction of the experimental measurements.

Summary

Since it is desirable that particles stay for a minimum defined time inside a calciner, to guarantee complete calcination, a target residence time with low axial dispersion is preferred. In this work, the influence of operational variables and material properties on the MRT, hold up, and axial dispersion was investigated in a pilot plant rotary calciner. The effects of operating conditions on the MRT and bed depth, similar to observations of previous work, were verified on the three kinds of alumina particles. Results showed that the MRT increase with a decrease in the incline angle and the rotary speed. The bed depth increased as the feed rate increased, while the effect of feed rate on the MRT was not significant. It was observed that spheres have lower residence time than cylinders and quadrulobes. This difference in residence time was correlated to the flowability of the material through measurement of the angle of repose of the material. The influence of material properties on the particle dispersion behavior was investigated captured in this work, which was not reported in previous literatures. The axial dispersion coefficient decreased with a decrease in rotary speed and incline angle. High feed rate and large angle repose of the materials led to high fill level and strong interactions between neighboring particles, which in turn led to limited axial dispersion.

Particle-size distribution or L/D ratio distribution are common in industrial materials; the influence of particle size and shape properties on the residence time distribution was also investigated in this article. It was observed that smaller or more slender particles stay longer time inside the calciner, leading to an axial segregation of materials. By applying the Saeman's model, a method was developed to provide reasonable RTD predictions in our calcination system for cylinders and quadrulobes. This method also led to good predictions for spheres at high feed rates.

As stated before, the performance of a continuous calciner is determined by the competition between the residence time

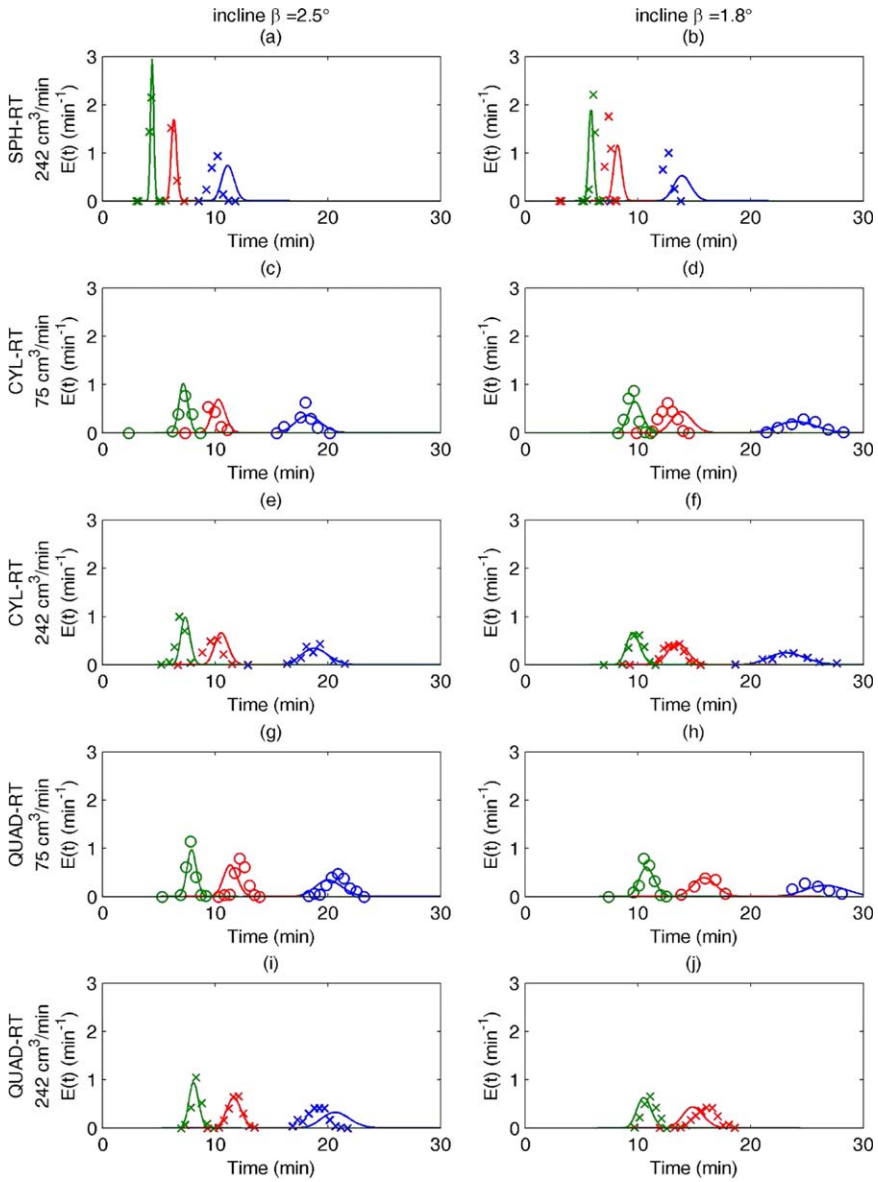

Figure 10. Prediction of RTDs at RT.

All cases are predicted except the sphere cases at low feed rate. [Color figure can be viewed in the online issue, which is available at wileyonlinelibrary.com].

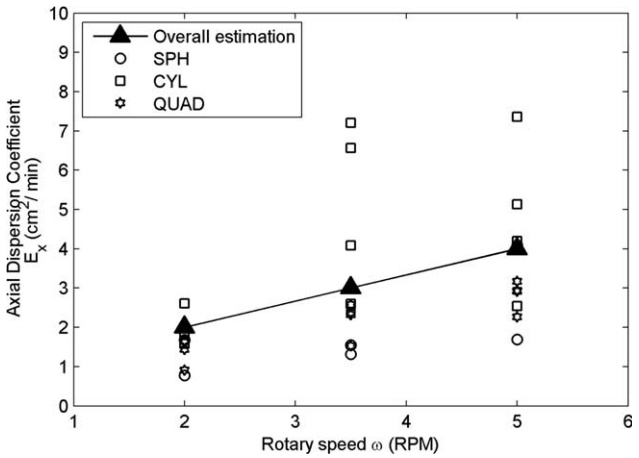

Figure 11. Estimation of the overall axial dispersion coefficient.

and the characteristic time of heat transfer in the transverse plane. As a result, the effect of temperature on the material flow in the calciner, as well as the cross-sectional heat-transport process, is suggested for further investigations. Coupling between the heat transfer and the axial particle flow and dispersion should also be considered.[5,39,40]

Acknowledgment

This work was partially supported by the Rutgers Catalyst Manufacturing Science and Engineering Consortium.

Notation

$C(t)$ = concentration of particles as a function of time
d = particle diameter, mm
E_x = axial dispersion coefficient, cm^2/min

$E(t)$ = residence time distribution, min^{-1}
$h(x)$ = depth of solid bed, mm
h_{dam} = height of dam at the discharge, mm
l = length between discharge and tracer injection, m
$\dot{m}$ = mass feed rate, g/min
M = mass hold-up in the calciner, kg
Pe = Peclet Number
R = radius of calciner, mm
t = time, min
v_x = mean axial velocity, cm/min
$\dot{V}$ = volumetric feed rate, cm^3/min
x = axial distance of discharge, m
β = incline angle of calciner, °
ξ = dimensionless location
ε_x = local fill angle of solids, °
ρ_s = dilated particle density, g/cm^3
τ = mean residence time, min
θ = dimensionless time
Θ = angle of repose, °
ω = rotary speed, RPM

Literature Cited

1. Barr P, Brimacombe J, Watkinson A. A heat-transfer model for the rotary kiln: Part I. pilot kiln trials. *Metall Mater Trans B*. 1989;20(3):391–402.
2. Liu X, Khinast JG, Glasser BJ. A parametric investigation of impregnation and drying of supported catalysts. *Chem Eng Sci*. 2008;63(18):4517–4530.
3. Sarkar R, Chatterjee S, Mukherjee B, Tripathi HS, Haldar MK, Das SK, Ghosh A. Effect of alumina reactivity on the densification of reaction sintered nonstoichiometric spinels. *Ceramics Int*. 2003;29(2):195–198.
4. Borgwardt RH. Calcination kinetics and surface area of dispersed limestone particles. *AIChE J*. 1985;31(1):103–111.
5. Ortiz OA, Suárez GI, Nelson A. Dynamic simulation of a pilot rotary kiln for charcoal activation. *Comput Chem Eng*. 2005;29(8):1837–1848.
6. Marias F, Roustan H, Pichat A. Modelling of a rotary kiln for the pyrolysis of aluminium waste. *Chem Eng Sci*. 2005;60(16):4609–4622.
7. Huang T-J, Yu T-C. Calcination conditions on copper/alumina catalysts for carbon monoxide oxidation and nitric oxide reduction. *Appl Catal*. 1991;71(2):275–282.
8. Barr P, Brimacombe J, Watkinson A. A heat-transfer model for the rotary kiln: Part II. Development of the cross-section model. *Metall Mater Trans B*. 1989;20(3):403–419.
9. Boateng AA, Barr PV. A thermal model for the rotary kiln including heat transfer within the bed. *Int J Heat Mass Transfer*. 1996;39(10):2131–2147.
10. Boateng AA, Barr PV. Modelling of particle mixing and segregation in the transverse plane of a rotary kiln. *Chem Eng Sci*. 1996;51(17):4167–4181.
11. Dhanjal S, Barr P, Watkinson A. The rotary kiln: an investigation of bed heat transfer in the transverse plane. *Metall Mater Trans B*. 2004;35(6):1059–1070.
12. Ding YL, Forster RN, Seville JPK, Parker DJ. Some aspects of heat transfer in rolling mode rotating drums operated at low to medium temperatures. *Powder Technol*. 2001;121(2–3):168–181.
13. Li SQ, Ma LB, Wan W, Yao Q. A Mathematical Model of Heat Transfer in a Rotary Kiln Thermo-Reactor. *Chem Eng Technol*. 2005;28(12):1480–1489.
14. Remy B, Khinast JG, Glasser BJ. Discrete element simulation of free flowing grains in a four-bladed mixer. *AIChE J*. 2009;55(8):2035–2048.
15. Conway SL, Glasser BJ. Density waves and coherent structures in granular Couette flows. *Phys Fluids*. 2004;16(3):509–529.
16. Chaudhuri B, Muzzio FJ, Tomassone MS. Experimentally validated computations of heat transfer in granular materials in rotary calciners. *Powder Technol*. 2010;198(1):6–15.
17. Chaudhuri B, Muzzio FJ, Tomassone MS. Modeling of heat transfer in granular flow in rotating vessels. *Chem Eng Sci*. 2006;61(19):6348–6360.
18. Thammavong P, Debacq M, Vitu S, Dupoizat M. Experimental apparatus for studying heat transfer in externally heated rotary kilns. *Chem Eng Technol*. 2011;34(5):707–717.
19. Liu XY, Specht E. Temperature distribution within the moving bed of rotary kilns: measurement and analysis. *Chem Eng Process: Process Intens*. 2010;49(2):147–150.
20. Sullivan JD, Macer CG, Ralston OC. Passage of solid particles through rotary cylindrical kilns. *US Bur Mines Techincal Pap*. 1927;384.
21. Saeman WC. Passage of solids through rotary kilns: factors affecting time of passage. *Chem Eng Prog*. 1951;47:508–514.
22. Kramers H, Croockewit P. The passage of granular solids through inclined rotary kilns. *Chem Eng Sci*. 1952;1(6):259–265.
23. Sai P, Surender G, Damodaran A, Suresh V, Philip Z, Sankaran K. Residence time distribution and material flow studies in a rotary kiln. *Metall Mater Trans B*. 1990;21(6):1005–1011.
24. Scott DM, Davidson JF, Lim SY, Spurling RJ. Flow of granular material through an inclined, rotating cylinder fitted with a dam. *Powder Technol*. 2008;182(3):466–473.
25. Liu XY, Zhang J, Specht E, Shi YC, Herz F. Analytical solution for the axial solid transport in rotary kilns. *Chem Eng Sci*. 2009;64(2):428–431.
26. Liu XY, Specht E. Mean residence time and hold-up of solids in rotary kilns. *Chem Eng Sci*. 2006;61(15):5176–5181.
27. Chen WZ, Wang CH, Liu T, Zuo CY, Tian YH, Gao TT. Residence time and mass flow rate of particles in carbon rotary kilns. *Chem Eng Process: Process Intens*. 2009;48(4):955–960.
28. Sudah OS, Chester AW, Kowalski JA, Beeckman JW, Muzzio FJ. Quantitative characterization of mixing processes in rotary calciners. *Powder Technol*. 2002;126(2):166–173.
29. Henein H, Brimacombe J, Watkinson A. The modeling of transverse solids motion in rotary kilns. *Metall Mater Trans B*. 1983;14(2):207–220.
30. Sherritt RG, Chaouki J, Mehrotra AK, Behie LA. Axial dispersion in the three-dimensional mixing of particles in a rotating drum reactor. *Chem Eng Sci*. 2003;58(2):401–415.
31. Ding YL, Seville JPK, Forster R, Parker DJ. Solids motion in rolling mode rotating drums operated at low to medium rotational speeds. *Chem Eng Sci*. 2001;56(5):1769–1780.
32. Liu XY, Specht E, Mellmann J. Slumping–rolling transition of granular solids in rotary kilns. *Chem Eng Sci*. 2005;60(13):3629–3636.
33. Heydenrych MD, Greeff P, Heesink ABM, Versteeg GF. Mass transfer in rolling rotary kilns: a novel approach. *Chem Eng Sci*. 2002;57(18):3851–3859.
34. Danckwerts PV. Continuous flow systems: distribution of residence times. *Chem Eng Sci*. 1953;2(1):1–13.
35. Levenspiel O, Smith WK. Notes on the diffusion-type model for the longitudinal mixing of fluids in flow. *Chem Eng Sci*. 1957;6(4-5):227–235.
36. Gao Y, Vanarase A, Muzzio F, Ierapetritou M. Characterizing continuous powder mixing using residence time distribution. *Chem Eng Sci*. 2011;66(3):417–425.
37. Risken H. *The Fokker-Planck Equation: Methods of Solution and Applications*, 2nd ed. New York: Springer; 1996.
38. Conway SL, Liu X, Glasser BJ. Instability-induced clustering and segregation in high-shear Couette flows of model granular materials. *Chem Eng Sci*. 2006;61(19):6404–6423.
39. Georgallis M, Nowak P, Salcudean M, Gartshore IS. Modelling the Rotary Lime Kiln. *Can J Chem Eng*. 2005;83(2):212–223.
40. Ferron JR, Singh DK. Rotary kiln transport processes. *AIChE J*. 1991;37(5):747–758.

Manuscript received Jan. 14, 2013, and revision received Jun. 6, 2013.